Expansion and shrinkage of lightweight vermiculite material at high temperatures

Petersen, Rasmus Rosenlund; Brandstrup Olesen, Martin ; König, J.; Yue, Yuanzheng

Published in:
Ceramics International

DOI (link to publication from Publisher):
10.1016/j.ceramint.2023.04.195

Publication date:
2023

Document Version
Publisher's PDF, also known as Version of record

Ceramics International 49 (2023) 23605–23611

Contents lists available at ScienceDirect

Ceramics International

journal homepage: www.elsevier.com/locate/ceramint

Expansion and shrinkage of lightweight vermiculite material at high temperatures

Rasmus R. Petersen [a,b,*], Martin B. Olesen [b], Jakob König [c], Yuanzheng Yue [b]

[a] R&D Department, Skamol A/S, DK-7860, Spøttrup, Denmark
[b] Department of Chemistry and Bioscience, Aalborg University, DK-9220, Aalborg Øst, Denmark
[c] Advanced Materials Department, Jožef Stefan Institute, Jamova Cesta 39, SI-1000, Ljubljana, Slovenia

ARTICLE INFO

Handling Editor: P. Vincenzini

Keywords:
Vermiculite
Expansion
Shrinkage
Potassium silicate

ABSTRACT

Vermiculite materials are widely used as insulation material in the industry, fire protection systems, and fire stoves. The high dimensional stability of vermiculite boards ensures that thermal runways in the insulation lining are avoided. Vermiculite boards for high-temperature applications are produced from thermally expanded vermiculite and alkali silicate binder. Here, we show the impact of potassium silicate binder and vermiculite source on the dimensional stability of vermiculite boards. The vermiculite boards expand at 500–830 °C and shrink stepwise at 1000–1250 °C and 1400 °C, respectively, when heated at 10 °C min^{-1} in ambient air. The expansion process is discussed in relation to the boards containing non-expanded particles and metal carbonates. The evolved gas analysis indicates that the CO_2 release from metal carbonates is the potential cause of the expansion of some vermiculite types. The shrinkage is initiated by the dehydroxylation of the clay structure. The binder promotes crystallisation during the shrinkage, ceasing the shrinkage process at higher temperatures. The expansion and shrinkage of vermiculite boards are anisotropic and depend on the board density and vermiculite origin. These findings provide new insights into the expansion and shrinkage behaviour of vermiculite boards.

1. Introduction

Vermiculite is a commodity name for a mineral mixture containing vermiculite (V), phlogopite (P), and interstratified phases of vermiculite and phlogopite (V–P). The interstratified phase with a 50:50 ratio of V and P is called hydrobiotite (or hydrophlogopite). Vermiculite exists as trioctahedral- and dioctahedral vermiculite, the former is commonly found in commercial deposits [1]. Vermiculite and interstratified V–P expand greatly when heated very fast at high temperatures (400–1000 °C). Here, we use the term "vermiculite" to cover the raw or processed mineral mixture and the term "vermiculite phase" for the specific vermiculite phase.

Expanded vermiculite can be used in fire protection [2–4], as soil amendments [5], as lightweight filling in concrete [6], as improver of membrane performance [3,7,8], as a matrix substance in energy storage systems [9], catalyst reactors [10], and heat insulation materials [11].

Vermiculite board is an insulation material with a working range from 25 to 1200 °C. They find primary use in the aluminium industry [11–13], wood stoves [14,15], and as passive fire protection [16], owing to its high thermal and dimensional stability, low thermal conductivity, excellent thermal shock resistance, and high chemical resistance. The manufacturing of vermiculite boards involves first an expansion of the vermiculite through flash heating and then mixing of expanded vermiculite with a binder. Sodium and potassium silicate are often applied as binders for board manufacturing [11]. Potassium silicate favours higher thermal stability. The mixture is finally shaped and hardened to form a monolithic lightweight material.

The dimensional stability of the insulation materials is crucial to keep a stable heat transfer through the insulation lining. For instance, if the insulation material shrinks, gaps are formed between the insulation units. If the material expands, cracks can form in the insulation material. Cracks and gaps function as thermal bridges and should be avoided to keep a low energy consumption. For these reasons, it is important to understand the mechanism behind dimensional changes in insulation materials [17–19].

There are several published reports on the thermal properties of vermiculite bonded materials. The dimensional changes of vermiculite bonded with geopolymer were studied during heating up to 1200 °C [20]. The mechanical properties of the cement bonded vermiculite were studied in the temperature range from room temperature to 1100 °C

* Corresponding author. R&D Department, Skamol A/S, DK-7860, Spøttrup, Denmark.
E-mail address: rp@bio.aau.dk (R.R. Petersen).

https://doi.org/10.1016/j.ceramint.2023.04.195
Received 8 October 2022; Received in revised form 24 March 2023; Accepted 24 April 2023
Available online 25 April 2023

[21]. A recent work reported on the chemical degradation of the vermiculite boards that were exposed to Na vapour at 970 °C [22]. In our earlier work [23], we reported on the phase changes occurring during the material processing and dynamic heating of potassium silicate-bonded vermiculite boards at high temperatures (25–1425 °C). This work focuses on explaining the dimensional changes occurring at elevated temperatures using heating microscopy and evolved gas analysis.

2. Materials & methods

2.1. Materials

All the vermiculite samples were of commercial grade and the particle size was between 0.355 and 1 mm. Vermiculite samples originated from the Palabora deposit (Limpopo, South Africa), Qieganbulake deposit (Xinjiang, China), and Karakoç deposit (Yıldızeli/Sivas, Turkey), hereafter named PV, QV, and KV, respectively. The vermiculite particles were thermally expanded in a gas-fired furnace (flash-heat treatment). More details are found in Ref. [23].

The expanded vermiculite was mixed with potassium silicate solution. The silicate solution was stored in closed containers and the shelf time of closed containers was approx. one week. The silicate solution was sprayed onto the expanded vermiculite particles while mixing. A mixture without silicate solution was prepared using the same procedure. The mixture was pressed uniaxially (Fig. 1a) to gain boards of 200 mm × 200 mm × 40 mm. The piston position was controlled within ±1 mm. The density was controlled by varying the mass. The boards were then dried at 120 °C for 16 h.

2.2. Characterisation

2.2.1. Chemical analysis

The chemical composition of the vermiculite (Table 1) was measured with an X-ray fluorescence spectrometer (Epsilon 3x, PANalytical) using the glass bead technique. Loss on ignition (LOI) was determined at 1030 °C. The uncertainty was below ±0.8 wt%.

2.2.2. Heating microscopy

The expansion behaviour of the raw vermiculite was analysed using a custom made heating microscope (Hesse Instruments). The thickness of the PV particles was 0.2 cm, and that of QV and KV particles was 0.3 cm. Randomly selected vermiculite particles (0.4 g) were placed inside a squared quartz tube with round edges, which was standing on an Al_2O_3 plate (Fig. 2). The central parts of the front and back surface of the tube were parallel to each other, allowing transmission of the light through the tube. The edges near the corners are curved and appear black in the heating microscope images, due to scattering. The vermiculite particles (V) lay flat on the surface of the Al_2O_3 plate. The sample silhouette height was measured from the recorded images. The sample height was measured at three positions. The heating microscope was equipped with a blue light and black/white camera with a telocentric lens. The samples were heated in air under ambient pressure at 10 °C min^{-1}.

The expansion and shrinkage of the boards were analysed with the heating microscope (Hesse Instruments). Samples of approximately 1 cm × 1 cm × 1 cm were sawed from larger samples (Fig. 1b). The samples were dried at 110 °C and cleaned with pressurised air before the measurement. The samples were placed on an Al_2O_3 plate and the sample surface, which was exposed to a pressing piston during the sample fabrication, turned upwards during heat treatment (Fig. 1c). The samples were heated at 10 °C min^{-1} in the air under ambient pressure. Images recorded with the camera were analysed with the EMI 3.0.1a software (Hesse Instruments). Only the sample silhouette was part of the image analysis (Fig. 2). The sample silhouette area (A) was determined by counting the black pixels of the sample. The sample height (H) was determined as the maximum sample height measured perpendicular to the base plate. The sample width (W) was determined as the maximum sample width measured parallel to the bottom of the image frame.

2.2.3. Phase analysis

Vermiculite and the vermiculite boards were measured with an X-ray diffractometer (Empyrean, PANalytical) to identify crystalline phases. Cu-Kα radiation at 45 kV and 40 mA was used. The diffractometer was equipped with a Ni-β filter, soller slit (0.04 rad), anti-scatter slit (1/8°), and divergence slit (1/16°) on the primary site and anti-scatter slit (11.2 mm) and soller slit (0.04 rad) on the secondary site. The diffracted beam was recorded with a PIXcel1D detector. The scanning range was 2.0–80° (2θ) and the diffractograms were scanned three times, each time for 1 h. The diffractograms reported are the sum of the three scans. All the samples were knife-milled and back-loaded onto the sample holder prior to the measurement. The phases were identified using Highscore Plus software (PANalytical) by comparing peak position and intensity with the PDF-2 database and with in-house reference minerals. The following references were used to identify phases in the samples: Vermiculite (in-house), hydrobiotite (in-house), phlogopite (in-house), apatite (PDF # 00-015-0876), calcite (PDF# 00-005-0586), dolomite (PDF# 00-011-0078), pyroxene (PDF# 01-070-2129).

2.2.4. Evolved gas analysis

Gasses evolved from the knife-grinded vermiculite boards were analysed using a Jupiter 449 simultaneous thermal analysis (STA) instrument coupled with a 403C Aëoloss mass spectrometer (MS)

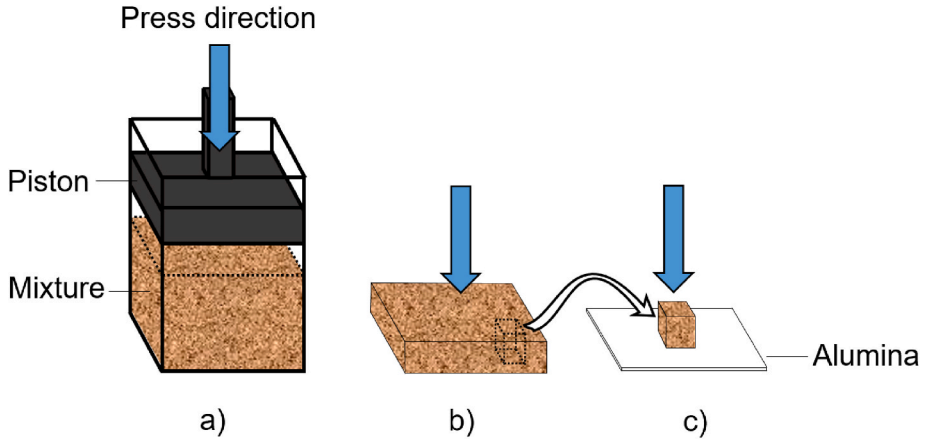

Fig. 1. a) A mixture of vermiculite and potassium silicate solution pressed uniaxially, b) for thermal analysis, small samples were cut from the hardened board, and c) measured with a heating microscope by placing the sample on an alumina plate with the press direction perpendicular to the alumina plate.

Table 1
Chemical composition of untreated vermiculite samples. The PV and QV compositions are from Ref. [23].

Oxide	SiO_2	TiO_2	Al_2O_3	MgO	Fe_2O_3	K_2O	CaO	Na_2O	P_2O_5	Mn_3O_4	LOI
PV	38.3	0.9	8.5	23.7	8.4	4.7	3.4	/	1.0	/	10.6
KV	38.1	2.1	15.9	14.7	13.1	4.1	4.3	0.1	/	0.2	7.3
QV	37.7	1.0	11.0	23.2	5.6	3.8	2.6	1.0	/	/	13.3

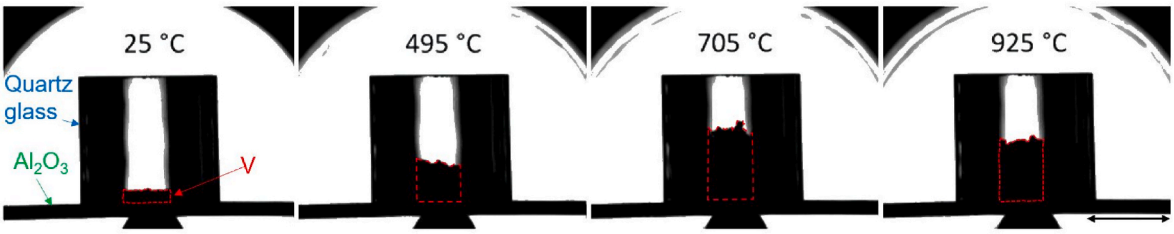

Fig. 2. Images of vermiculite particles (V) recorded with a heating microscope at 10 °C min^{-1}. The particles are located on a base plate (Al_2O_3) and surrounded by the surfaces of a quartz glass tube. The scale in the right bottom corner corresponds to 1 cm.

(Netzsch, Selb, Germany). The measurements were performed in the temperature range of 30–1250 °C with a heating rate of 10 °C min^{-1} in a flushing oxidizing atmosphere ($Ar/O_2 = 80/20$). The sample (20–25 mg) was inserted into an uncovered alumina crucible. The gases released from the inspected sample were detected by the MS.

2.2.5. *Flash heating*

A Bunsen burner with propane gas was used to heat the surface of the vermiculite boards. The boards were qualitatively checked for expanding vermiculite particles.

3. Results & discussion

3.1. *Vermiculite*

Phase analysis of the vermiculite samples (Fig. 3) shows that they have reflections of the vermiculite phase at 6.1° (14.4 Å), phlogopite at 8.7° (10 Å), and interstratified phases of vermiculite-phlogopite (V–P) at 6.5–8.0° (13.6–11.0 Å). The vermiculite phase corresponds to Mg-intercalated vermiculite (14.4 Å) with a double water layer hydration state (2-WLHS). The reflections centred around 7.0–7.7° (11.5–12.3 Å) indicate hydrobiotite (50-50, V–P). The peak broadening can be a result of different stacking sequences of vermiculite and phlogopite phases, and variations of hydration states. Minor amounts of calcite ($CaCO_3$) and amphibole are detected from the XRD patterns. Apatite is also detected in the PV sample. Detailed information on the PV sample is found in Refs. [24–26].

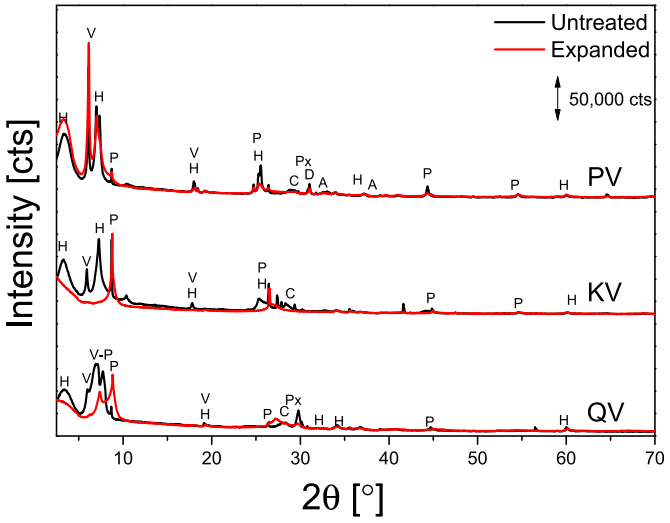

Fig. 3. X-ray diffractograms of untreated and expanded vermiculite. The letters refer to phases of vermiculite (V), hydrobiotite (H), interstratified vermiculite-phlogopite (V–P), phlogopite (P), apatite (A), pyroxene (Px), calcite (C), dolomite (D).

3.1.1. *Thermal expansion – flash heating*

Heating of vermiculite particles at high temperatures (~770 °C) for a very short time (~1 s) causes the particles to expand perpendicular to their basal planes. The loose bulk density of the particles decreases dramatically during the expansion process (Table 2).

The thermal expansion process changes the reflections of vermiculite and interstratified V–P phases to collapse irreversibly to 8.7° (~10 Å) with nearly the same interlayer distance as phlogopite (Fig. 3). The reflection is much broader than phlogopite, reflecting a distribution of different WLHS. The same change occurs for untreated vermiculite and pure vermiculite phase (see references in Ref. [23]). Suquet et al. [27] proposed that this event was caused by the formation of enstatite between the interlayers, thereby linking the interlayers together with covalent bonds. This prevents interlayers from reabsorbing moisture again. The expansion ability of vermiculite is discussed in detail elsewhere [23,28].

3.1.2. *Thermal expansion – dynamic heating*

The expansion of untreated vermiculite during dynamic heating (10 °C min^{-1}) is shown in Fig. 4. The expansion ability is lower compared to the case where the particles are flash heated. KV, QV, and PV samples start to expand around 250 °C. At higher temperatures, the expansion accelerates at 300 °C, 350 °C, and 420 °C for KV, QV, and PV, respectively. Particle size and interlayer ion influence the expansion ability. Interlayer sodium ions (Na^+) reduce the onset of expansion significantly [29]. As seen from Table 2, sodium is present in the QV sample. This can explain why the QV sample has a lower temperature of accelerated expansion. The KV sample exhibits also a low expansion temperature, however, the Na content in the KV sample is low. Particles

Table 2
Loose bulk density of untreated ($\rho_{untreated}$) and expanded ($\rho_{expanded}$) vermiculite and the expansion ratio ($K = \rho_{expanded}/\rho_{untreated}$).

Vermiculite	$\rho_{untreated}$	$\rho_{expanded}$	K
	[kg m^{-3}]	[kg m^{-3}]	[−]
PV	1062 ± 25	84 ± 2	12.6 ± 0.3
KV	564 ± 4	91 ± 5	6.2 ± 0.4
QV	849 ± 40	125 ± 24	6.9 ± 1.3

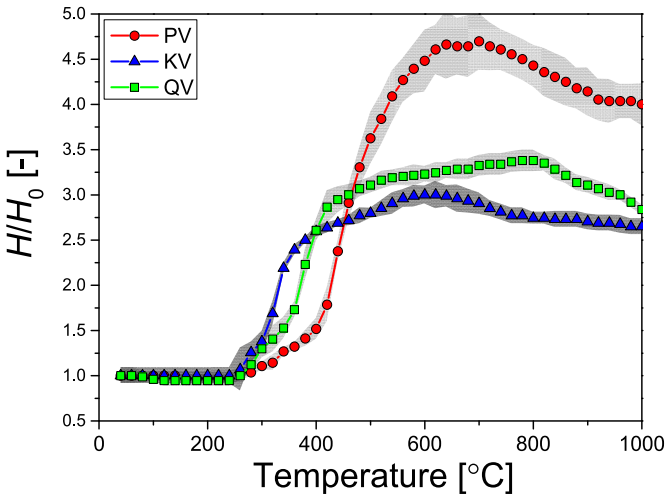

Fig. 4. Normalised sample height (H/H_0) of untreated vermiculite samples of different origins (PV, QV, KV) on dynamic heating at 10 °C min^{-1}. The hatched areas represent the standard deviations.

with multiple phases are likely to exhibit a lower onset temperature of expansion. Phlogopite can block the vapours escaping from the vermiculite phase or V–P, allowing vapour pressure to build up.

A lower onset expansion temperature of the PV vermiculite is observed by the heating microscope compared to that measured with a thermo-mechanical analyser (TMA) [29]. The TMA was measured on smaller particles (Micron grade) than the heating microscope (Super Fine grade). This illustrates the importance of particle size effect for the onset expansion temperature. PV, KV, and QV are of Super Fine grade and the sieve analysis (results not shown) indicated similar distribution. The difference in the expansion profiles between 300 and 400 °C is likely a combined effect of different phase compositions and interlayer cations.

3.2. Thermal stability of vermiculite boards

The vermiculite boards undergo a drastic change in their dimenions when being heated (Fig. 5). At 400–850 °C, the boards expand. From 1000 to 1200 °C, the boards shrink. From 1200 to 1300 °C, the boards start to shrink a second time. Each event is discussed separately below.

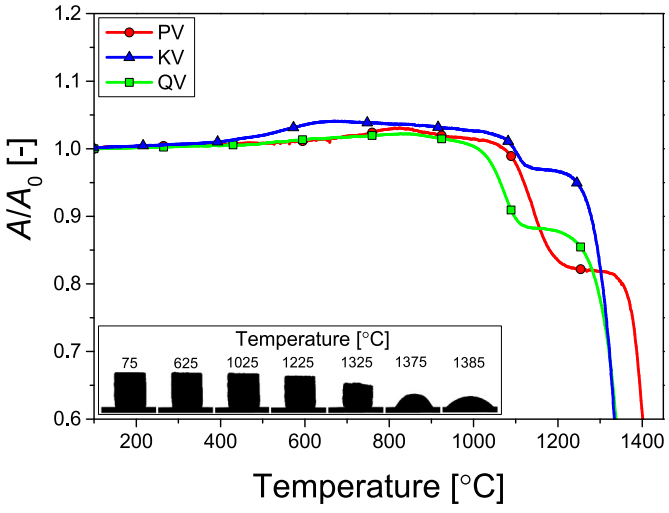

Fig. 5. Normalised silhouette area (A/A_0) of vermiculite boards heated at 10 °C min^{-1}. The inset contains images of the silhouette of a KV vermiculite board recorded at different temperatures.

3.2.1. Expansion

Vermiculite boards expand from room temperature up to 700–850 °C. The expansion accelerates for KV and PV at 400 °C and 700 °C, respectively, whereas the QV sample expands only slightly in comparison.

The vermiculite particles in the boards consist of flakes. The large flake surface orientates preferably in the press direction in which the boards were produced (Fig. 1a). Untreated vermiculite flakes expand in the *C-axis direction and since the *C-axis is preferably oriented parallel to the press direction, the expansion of vermiculite particles during dynamic heating should occur in the press direction. Fig. 6 shows the dimensional change of the KV vermiculite board in both the vertical (height, H/H_0) and horizontal (width, W/W_0) direction. The samples exhibit higher expansion in the press direction. This suggests that the expansion event of vermiculite boards is dominated by the expansion of water-rich interlayers, which could originate from partially or completely untreated vermiculite particles.

The potassium silicate binder becomes fluid around 500 °C [23] and the binder is therefore mobile when the vermiculite boards expand (400–700 °C). The vapours released from the dehydroxylation of the clay structure could potentially cause the foaming of the liquid potassium silicate and the expansion of the vermiculite board. In addition, potassium silicate can convert into K_2CO_3 [30] even at room temperature [31]. K_2CO_3 decomposes at ~820 °C when heated at 10 °C min^{-1} [32]. The CO_2 formed during the K_2CO_3 decomposition could cause an expansion of the samples. The temperature of decomposition (~820 °C) agrees well with the temperature of expansion (830 °C) of the PV sample. However, this mechanism fails to explain why the KV and the QV sample does not exhibit the similar expansion ability at 830 °C as the PV sample. Boards made without the binder show a similar expansion profile compared to those boards made with the binder (Fig. 7), suggesting that the expansion phenomena are related to the vermiculite particles.

Heating PV boards to 824 °C, followed by cooling to room temperature and then heating the board sample a second time to 824 °C reveals that the expansion occurring during the first and second heating is different (Fig. 8). The expansion during the first heating is close to exponential, whereas the expansion during the second heating is close to linear. This demonstrates that the expansion occurring during the first heating is irreversible.

The expansion profile of the vermiculite materials depends on the vermiculite origin [23]. Boards made from Karakoc vermiculite (KV) expand at 500 °C, whereas boards made from Palabora vermiculite (PV) have a major expansion at 830 °C. Remnants of untreated vermiculite particles could cause such expansion, however, the initial expansion profile of PV, QV, and KV particles (Fig. 4) does not agree with the dynamic expansion profile of the corresponding vermiculite boards (Fig. 5). The PV, KV, and QV particles contain different phases, as described before. Each particle consists of one or more phases. Particles with a mosaic distribution of phases gain the highest expansion ability [28]. Non-expandable phases block the vapour escape route, thereby inducing pressure build-up to the point of spontaneous expansion. Monophase particles with trioctahedral vermiculite contain the highest amount of water. Endothermic evaporation works against the temperature increase during the flash-heating. This increases the chance that the particles are processed without expansion. Those particles with a monophase of trioctahedral vermiculite have the highest endothermic capacity and therefore have the highest probability to avoid expansion.

Using a flame torch to flash-heat the pressed surface of a KV, PV, and QV vermiculite board for 3–5 s causes individual particles to expand from the board. Those expanding particles are dominated by those having a shiny goldish lustre. The phase composition of these particles is dominated by pure vermiculite phases, which do not expand during the thermal expansion process. This could be due to three reasons. First, they contain a high amount of interlayer water. The water provides a cooling effect on the particles, thereby preventing the vermiculite to

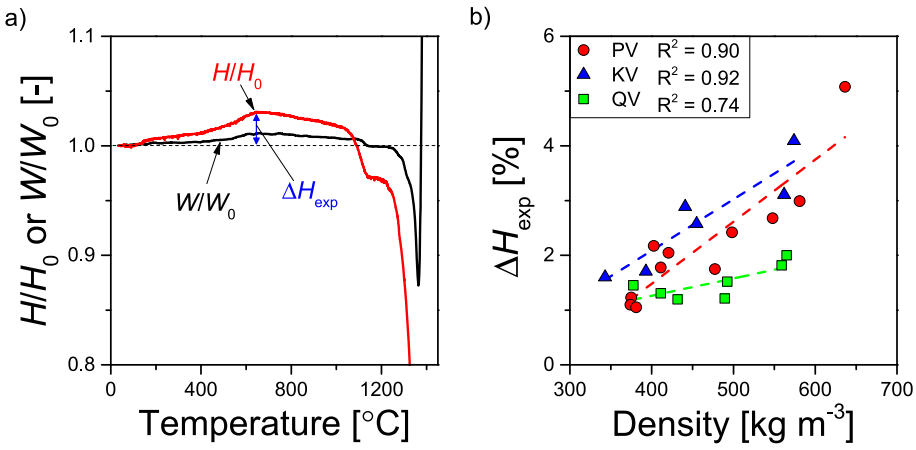

Fig. 6. a) Normalised sample height (H/H_0) and sample width (W/W_0) of KV vermiculite board with a density of 562 kg m^{-3}. b) Degree of expansion (ΔH_{exp}) of PV, KV, and QV vermiculite boards. The dashed lines are linear fits of the data.

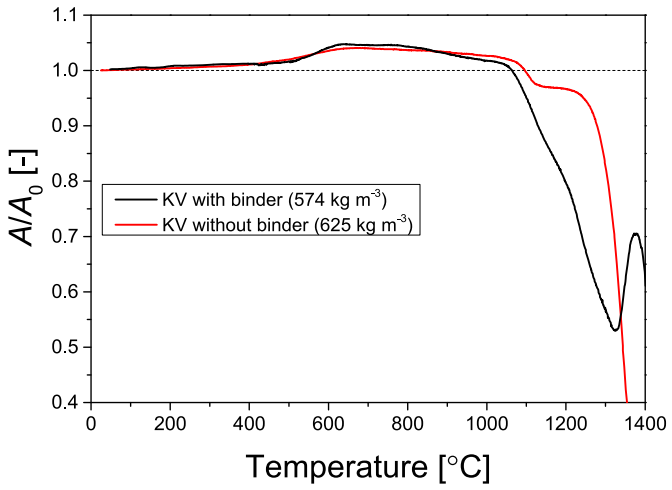

Fig. 7. Normalised area (A/A_0) of KV vermiculite board heated at 10 °C min^{-1}.

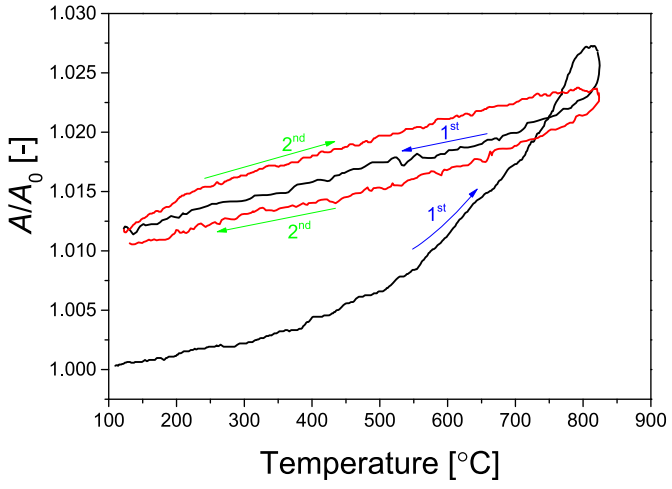

Fig. 8. Area of PV sample (A) normalised to the area at 100 °C (A_0). The sample is heated and cooled twice, as indicated by the arrows.

reach a sufficiently high temperature for expansion. Second, the particles have a high phase homogeneity, which allows the vapour in the interlayer to escape easily from all sides, thereby preventing critical pressure to build up. Third, the expansion process is short, allowing a short time for phase change and expansion. Hence, those particles with high content of vermiculite phases pass the flash-heating process without changing the phase. Even though the vermiculite phase dehydrates during the expansion process, the vermiculite phase rehydrates after heat treatment. Therefore, the non-expanded particles cause the expansion of the vermiculite board as observed by the heating microscope (Fig. 5). Following this mechanism, the expansion should increase with an increasing amount of non-expanded particles. The number of non-expanded particles increases as the board density increases. Hence, the role of non-expanded particles can explain why the expansion is dependent on the density.

3.2.2. *Evolved gas analysis*

Evolved gas analysis on vermiculite boards observed using mass spectroscopy shows a strong signal of mass-to-charge ratio (m/z) of 18 and 44 (Fig. 9), which correspond to H_2O and CO_2, respectively. H_2O

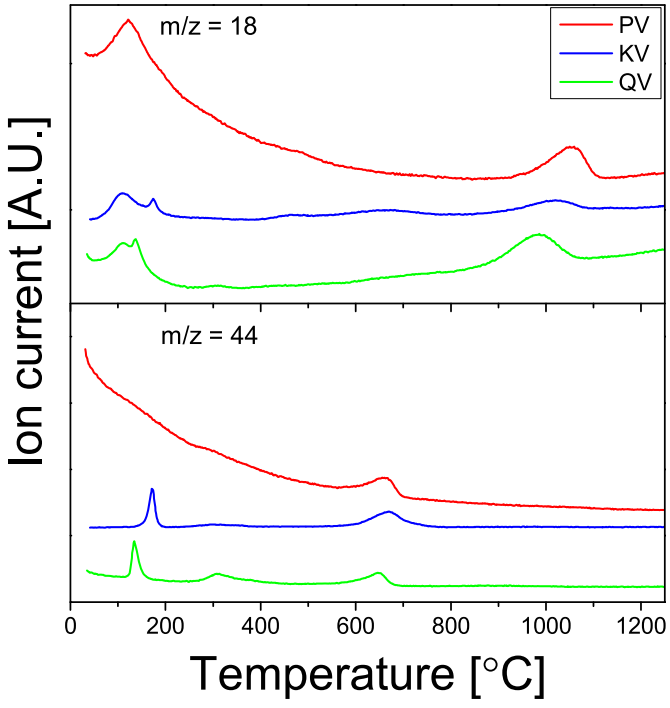

Fig. 9. Ion current obtained from mass spectroscopy of gasses released from ground vermiculite boards. Charged species of H_2O and CO_2 correspond to the mass-charge ratio (m/z) of 18 and 44, respectively.

and CO_2 are the main gases. Other gases (e.g. HCl, SO_2) are only found in trace amounts. The CO_2 peak at 150–200 °C could be due to physically adsorbed CO_2 on the surface, which is released at <250 °C from silicate surfaces [33]. A minor CO_2 release occurs at 300 °C, which can be attributed to burn-out of organic material. At 600–700 °C, minor content of metal carbonates (calcite/dolomite) decompose and release CO_2 [23,26]. Carbonate minerals located inside the clay particles [26] could potentially cause the expansion of the particles during the thermal decomposition of the carbonates. When dripping acid on the expanded vermiculite a strong bubble evolution is observed [23]. This indicates that metal carbonates (calcite and dolomite) are present in the expanded vermiculite.

The onset temperature of expansion for PV, KV, and QV is 720, 535, and 790 °C, respectively. The expansion temperatures of PV and QV boards are similar and can be related to carbonate minerals in the following way. When the CO_2 gas is released in the boards, the gasses are retained in the board before the CO_2 can diffuse through the board and escape to the atmosphere. The continuous increase in temperature causes a thermal expansion of entrapped CO_2 gasses, thereby expanding the board. The diffusion path is longer in the bulk samples (1 cm^3) used for the heating microscopy than in the ground samples used for evolved gas analysis. Therefore, the expansion onset of boards in the heating microscope exhibits a time lag compared to the apparent onset temperature of CO_2 emission. Following this mechanism, the expansion ability is dependent on the density, as seen in Fig. 6b. The KV sample expands at lower temperatures (535 °C) compared to the PV and QV sample (720–790 °C). This can be ascribed to the expansion of clay particles, which increases the porosity of the board and opens the structure. This enables a faster escape of CO_2, when the metal carbonate decomposes at higher temperatures (600–700 °C). Hence, the KV board does not show expansion in the similar temperature range as the PV and QV.

The H_2O emission at 25–200 °C corresponds to the loss of the interlayer water from clay particles [23,34], free water, adsorbed water, and hydroxyl groups from the potassium silicate surface [23,35,36]. The H_2O emission at 825–1100 °C corresponds to the dehydroxylation of clay minerals.

3.2.3. Shrinkage

At 1000–1250 °C, the vermiculite boards undergo a major shrinkage (Fig. 5). During this event, the crystalline phase composition changes from dehydrated vermiculite and hydrobiotite phases to forsterite and leucite [20,23]. Boards prepared without the binder exhibit a similar onset temperature of shrinkage (Fig. 7), however, further heating only increases the degree of shrinkage. Boards without the binder form forsterite during shrinking but no leucite is formed. This suggests that the potassium silicate binder induces a fast crystallisation into leucite, which halts the shrinkage process during dynamic heating.

The onset shrinkage temperature depends on the vermiculite origin but is independent of density [23]. The shrinkage process and the phase transformation into forsterite and leucite follow, subsequently, the dehydroxylation process. The low dehydroxylation temperature of the QV board (Fig. 9) agrees well with the low onset temperature of shrinkage (Fig. 5). The dehydroxylation temperature of sheet silicates is affected by the trioctahedral environment [37,38]. Differences in the trioctahedral environment could explain the different shrinkage temperatures. Walker & Cole [34] suggested that a high $Si:Al^{IV}$ ratio of the tetrahedral layers resulted in higher thermal stability of vermiculite. This could explain the different shrinkage temperatures of PV and QV. However, the KV sample has the lowest $Si:Al^{IV}$ ratio, but exhibit a high onset shrinkage temperature.

The second shrinkage event of vermiculite boards (1290–1380 °C) is related to the melting of leucite, whereas forsterite seems to remain stable up to 1425 °C [23].

Future research will focus on determining the phase composition and structural formulas of untreated vermiculite. It is important to establish a link between the crystal chemistry of untreated vermiculite and the thermal properties of the potassium silicate bonded vermiculite materials.

4. Conclusions

Vermiculite boards were made from expanded vermiculite and potassium silicate binder. The vermiculite particles were expanded through a flash heat treatment. Vermiculite boards under went expansion and shrinkage during dynamic heating. The expansion process was irreversible and anisotropic, i.e., the boards exhibited greater expansion in the direction in which they were pressed into boards.

The expansion ability is dependent on the density and origin of the vermiculite source. The onset temperature of expansion depends on the vermiculite origin. The expansion mechanism was discussed in relation to binder and mineral phases. Binder had no influence on the expansion ability, since material without binder expands to a similar extent. The results suggests that the clay particles cause expansion at low temperatures (535 °C) and metal carbonate are responsible for the expansion at higher temperatures (720–790 °C).

At 1000–1250 °C, the boards shrink anisotropically due to dehydroxylation. The binder induces crystallisation during the shrinkage. The new crystalline phases prevent further shrinkage and stabilises the shrinking process up to 1250–1350 °C.

Declaration of competing interest

The authors declare that they have no known competing financial interests or personal relationships that could have appeared to influence the work reported in this paper.

Acknowledgement

This work was supported by Innovationsfonden (Case no. 7039-00042B).

References

[1] Deer, Howie, Zussman, in: M.J. Wilson (Ed.), Rock-Forming Minerals: Sheet Silicates: Clay Minerals 3C, The Geological Society, 2013, 2nd.
[2] G. Landucci, M. Molag, V. Cozzani, Modeling the performance of coated LPG tanks engulfed in fires, J. Hazard Mater. 172 (2009) 447–456, https://doi.org/10.1016/j.jhazmat.2009.07.029.
[3] M. Carter, M.H. Parekh, V. Tomar, J.E. Dietz, V.G. Pol, Flame retardant vermiculite coated on polypropylene separator for lithium-ion batteries, Appl. Clay Sci. 208 (2021), 106111, https://doi.org/10.1016/j.clay.2021.106111.
[4] C.T. Long, R. Wang, C. Shoalmire, D.S. Antao, P.J. Shamberger, J.C. Grunlan, Efficient heat shielding of steel with multilayer nanocomposite thin film, ACS Appl. Mater. Interfaces 13 (2021) 19369–19376, https://doi.org/10.1021/acsami.1c03781.
[5] J.-Y. Kang, H.-H. Lee, K.-H. Kim, Physical and chemical properties of inorganic horticultural substrates used in Korea, Acta Hortic. (2004) 237–241, https://doi.org/10.17660/ActaHortic.2004.644.32.
[6] F. Koksal, Y. Sahin, O. Gencel, Influence of expanded vermiculite powder and silica fume on properties of foam concretes, Construct. Build. Mater. 257 (2020), 119547, https://doi.org/10.1016/j.conbuildmat.2020.119547.
[7] K. Huang, P. Rowe, C. Chi, V. Sreepal, T. Bohn, K.G. Zhou, Y. Su, E. Prestat, P. B. Pillai, C.T. Cherian, A. Michaelides, R.R. Nair, Cation-controlled wetting properties of vermiculite membranes and its promise for fouling resistant oil–water separation, Nat. Commun. 11 (2020) 1–10, https://doi.org/10.1038/s41467-020-14854-4.
[8] T. Liu, C. Zhang, J. Yuan, Y. Zhen, Y. Li, Two-dimensional vermiculite nanosheets-modified porous membrane for non-aqueous redox flow batteries, J. Power Sources 500 (2021), 229987, https://doi.org/10.1016/j.jpowsour.2021.229987.
[9] R. Fisher, Y. Ding, A. Sciacovelli, Hydration kinetics of K2CO3, MgCl2 and vermiculite-based composites in view of low-temperature thermochemical energy storage, J. Energy Storage 38 (2021), 102561, https://doi.org/10.1016/j.est.2021.102561.
[10] M. Reli, N. Ambrožová, M. Valášková, M. Edelmannová, L. Čapek, C. Schimpf, M. Motylenko, D. Rafaja, K. Kočí, Photocatalytic water splitting over CeO2/Fe2O3/Ver photocatalysts, Energy Convers. Manag. 238 (2021), https://doi.org/10.1016/j.enconman.2021.114156.
[11] A. Yurkov, Refractories for Aluminium: Electrolysis and the Cast House, Springer, 2015.

[12] A.T. Tabereaux, Thermal insulation materials for reduction cell cathodes, in: J. Andersen, A. Tomsett (Eds.), Essent. Readings Light Met., Springer, The Minerals, Metals & Materials Society, 1982, pp. 876–887.
[13] J.B.B. Frandsen, L.F. Juhl, Isoleringsplade Til Brug Ved Foring Af Forme for Aggressive Smeltede Metealler Og Fremgangsmåde Til Fremstilling Af Isolreingspladen Samt Anvendelse Af Denne, DK160149B, Danish Patent), 1985.
[14] C.R. Chaplin, Wood burning stoves: material selection and thermal shock testing of fired ceramic bodies, Proc. Indian Acad. Sci. Sect. C Eng. Sci. 6 (1983) 47–58, https://doi.org/10.1007/BF02843290.
[15] T. Kristensen, S.N. Bertel, Catalytic Unit for Solid Fuel Burning Stoves, Canadian patent), 2013. CA2871526A1.
[16] J. Becker, Formteil für Brandschutz und Verfahren zur Herstellung eines Formteils, German patent), 2007. DE102007026970A1.
[17] Ë.V. Degtyareva, M.M. Martynenko, A.N. Gadou, E.I. Zoz, Reduction of linear shrinkage in glass-fiber refractories during service, Sci. Res. (1983) 3–7, https://doi.org/10.1007/BF01398748.
[18] M. Jensen, M.M. Smedskjaer, Y. Yue, Diffusion limited dissolution of an MgO layer on basaltic glass fibres, Phys. Chem. Glas. Eur. J. Glas. Sci. Technol. Part B. 52 (2011) 187–192.
[19] N. Takahashi, S. Hashimoto, Y. Daiko, S. Honda, Y. Iwamoto, High-temperature shrinkage suppression in refractory ceramic fiber board using novel surface coating agent, Ceram. Int. 44 (2018) 16725–16731, https://doi.org/10.1016/j.ceramint.2018.06.100.
[20] V. Medri, E. Papa, M. Mazzocchi, L. Laghi, M. Morganti, J. Francisconi, E. Landi, Production and characterization of lightweight vermiculite/geopolymer-based panels, Mater. Des. 85 (2015) 266–274, https://doi.org/10.1016/j.matdes.2015.06.145.
[21] F. Koksal, K. Cos, M. Dener, A. Benli, O. Gencel, Insulating and Fire-Resistance Performance of Calcium Aluminate Cement Based Lightweight Mortars, 2023, p. 362, https://doi.org/10.1016/j.conbuildmat.2022.129759.
[22] R. Luneng, S.N. Bertel, J. Mikkelsen, A.P. Ratvik, T. Grande, Chemical durability of thermal insulating materials in Hall-héroult electrolysis cells, Ceramics 2 (2019) 441–459, https://doi.org/10.3390/ceramics2030034.
[23] R.R. Petersen, J.F.S. Christensen, N.T. Jørgensen, S. Gustafson, L.A. Lindbjerg, Y. Yue, Preparation and thermal properties of commercial vermiculite bonded with potassium silicate, Thermochim. Acta 699 (2021), 178926, https://doi.org/10.1016/j.tca.2021.178926.
[24] G.A. Swayze, H.A. Lowers, W.M. Benzel, R.N. Clark, R.L. Driscoll, Z.S. Perlman, T. M. Hoefen, M.D. Dyear, Characterizing the source of potentially asbestos-bearing commercial vermiculite insulation using in situ IR spectroscopy, Am. Mineral. 103 (2018) 517–549, https://doi.org/10.2138/am-2018-6022.
[25] C. Marcos, I. Rodríguez, Applied clay science expansion behaviour of commercial vermiculites at 1000 ° C, Appl. Clay Sci. 48 (2010) 492–498, https://doi.org/10.1016/j.clay.2010.02.012.
[26] R. Kikuchi, T. Kogure, Structural and compositional variances in 'hidrobiotite' sample from palabora, South Africa, Clay Sci. 22 (2018) 39–52, https://doi.org/10.11362/jcssjclayscience.22.2_39.
[27] H. Suquet, C. Mallard, M. Quarton, J. Dubernat, H. Pezerat, Etude du biopyribole formé par chauffage des vermiculites magnésiennes, Clay Miner. 19 (1984) 217–227, https://doi.org/10.1180/claymin.1984.019.2.08.
[28] S. Hillier, E.M.M. Marwa, C.M. Rice, On the mechanism of exfoliation of 'Vermiculite, Clay Miner. 48 (2013) 563–582, https://doi.org/10.1180/claymin.2013.048.4.01.
[29] H.F. Muiambo, W.W. Focke, M. Atanasova, I. van der Westhuizen, L.R. Tiedt, Thermal properties of sodium-exchanged palabora vermiculite, Appl. Clay Sci. 50 (2010) 51–57, https://doi.org/10.1016/j.clay.2010.06.023.
[30] B. Sutens, Y. De Vos, B. Verougstraete, J.F.M. Denayer, M. Rombouts, Potassium silicate as low-temperature binder in 3D-printed porous structures for CO_2 separation, ACS Omega 8 (2023) 4116–4126, https://doi.org/10.1021/acsomega.2c07074.
[31] A. Sanna, M.M. Maroto-valer, Potassium based sorbents from fly ash for high temperature CO_2 capture, Environ. Sci. Pollut. Res. 23 (2016) 22242–22252, https://doi.org/10.1007/s11356-016-6378-x.
[32] P. Victor, S. Kim, J. Yoo, S. Lee, R. Youngjoon, J. Lim, S. Kim, D. Chun, K. Choi, Y. Rhee, Deactivation behavior of K2CO3 catalyst in the steam gasification deactivation behavior of K2CO3 catalyst in the steam, Trans. Korean Hydrog. New Energy Soc. 27 (2016) 517–525, https://doi.org/10.7316/KHNES.2016.27.5.517.
[33] J.F. Antonini, G. Hochstrasser, Surface states of pristine silica surfaces II. UHV studies of the CO2 adsorption-desorption phenomena, Surf. Sci. 32 (1972) 665–686, https://doi.org/10.1016/0039-6028(72)90193-8.
[34] G.F. Walker, W.F. Cole, The vermiculite minerals, in: R.C. Mackenzie (Ed.), Differ. Therm. Investig. Clays, Mineralogical Society (Clay Minerals Group), London, 1957, pp. 191–206.
[35] K.B. Langille, D. Nguyen, J.O. Bernt, D.E. Veinot, M.K. Murthy, Mechanism of dehydration and intumescence of soluble silicates - Part I Effect of silica to metal oxide molar ratio, J. Mater. Sci. 26 (1991) 695–703, https://doi.org/10.1007/BF00588306.
[36] H. Mohsin, E. Burov, S. Tusseau-nenez, S. Maron, L. Devys, T. Gacoin, E. Gouillart, Crystallization-induced suppression of intumescence in aqueous alkali silicates, J. Am. Ceram. Soc. (2022) 1–18, https://doi.org/10.1111/jace.18711.
[37] W. Smykatz-Kloss, Differential thermal analysis of Mg-bearing carbonates and sheet silicates, J. Therm. Anal. Calorim. 69 (2002) 85–92, https://doi.org/10.1023/A:1019933622550.
[38] J.M. Serratosa, J.A. Rausell-Colom, Dehydroxylation of micas and vermiculites. The effect of octahedral composition and interlayer saturating cations, Mineral. Petrogr. Acta 29-A (1985) 399–408.